Glancing interactions between single and intersecting oblique shock waves and a turbulent boundary layer

By D. J. MEE, R. J. STALKER AND J. L. STOLLERY†

University of Queensland, Brisbane, Australia

(Received 16 May 1985 and in revised form 13 March 1986)

The three-dimensional interactions of weak swept oblique shock and expansion waves and a turbulent boundary layer on a flat plate are investigated. Upstream influences in a single swept interaction are found to be consistent with a model of the flow involving shock/boundary-layer interaction characteristics. The model implies that there is more rapid thickening of the boundary layer close to the shock generator and this is seen to be consistent with surface streamline patterns. It is also found that a superposition principle, which is inherent in the triple-deck model of shock/boundary-layer interactions proposed by Lighthill, can be used to predict the pressure field and surface streamlines for the case of intersecting shock interactions and for the intersection of a shock with a weak expansion.

1. Introduction

The 'triple-deck' theory of shock/boundary-layer interaction involves a model of the interaction flow field in which the mainstream is taken as the outer deck, and the boundary layer is represented by a rotational inviscid flow as the middle deck, together with a viscous incompressible flow as the inner deck. The three-layer model is illustrated in figure 1. This was originally introduced by Lighthill (1953), who used it to develop an analytical theory of two-dimensional interaction with a supersonic mainstream. The theory was based on the assumption that all flow disturbance quantities were small compared with their corresponding values upstream of the interaction.

The model has subsequently proved to have a surprisingly wide range of applications to shock/boundary-layer interaction problems. For example, Stalker (1960) showed that it could be readily extended to apply to swept cylindrically symmetric interactions. Then, Stewartson & Williams (1969) used the theory to study two-dimensional interactions involving laminar boundary layers with separation, and concluded that large flow disturbances in the inner deck could be accommodated within the theory. Next, in an investigation of transonic normal-shock-wave/turbulent-boundary-layer interaction, Inger & Mason (1976) showed that it could also cope satisfactorily with the presence of a subsonic outer deck downstream of the shock wave, and Inger (1980) modified it to include turbulent shear stresses. Analyses involving matched asymptotic expansions have also used it for laminar boundary layers and in a modified form for turbulent layers (Adamson & Messiter 1980). Finally, returning to three-dimensional interactions, Stalker (1984) employed it to predict the manner in which spanwise disturbances would propagate in a swept interaction.

† Permanent address: College of Aeronautics, Cranfield Institute of Technology, Bedford, UK.

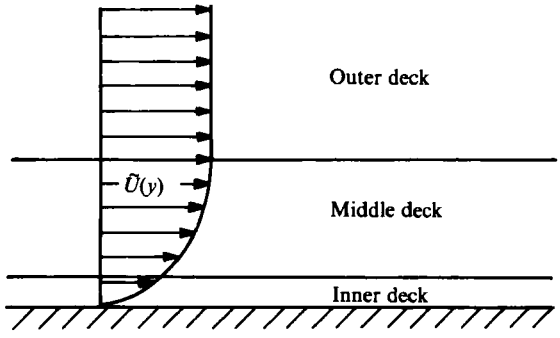

FIGURE 1. The triple-deck model.

Glancing interaction is one of the most important types of three-dimensional interference, in which an oblique shock wave crosses the path of a boundary layer growing along an adjacent wall. Although it has invariably been studied in the past with only one shock wave (e.g. Oskam, Bogdonoff & Vas 1975; Dolling & Bogdonoff 1981; Kubota & Stollery 1982), there are many situations in which two such shock waves intersect. This is likely to occur, for example, in supersonic engine intakes, turbine cascades, or between missile or aircraft fins.

Thus the work reported here is directed towards a study of the intersecting-shock case. However, as a preliminary step, it was necessary to understand the nature and development of the single oblique shock interaction more thoroughly, particularly in respect of surface flow directions. This has led to some new insight into that interaction. The two major parts of this paper are presented in §§3 and 4. Section 3 deals with the nature of a swept-shock-wave/boundary-layer interaction. The analysis of Stalker (1984), which shows that flow properties upstream of the shock can be treated in terms of a series of parallel characteristics, is investigated in the light of a new set of experimental results. A further model for the development of the interaction, consistent with available experimental data, is proposed. Section 4 investigates the validity of superposition of two single-shock-wave/boundary-layer interaction flow fields to predict the flow field obtained in the case of colliding swept interactions. Shock/shock and shock/expansion interactions are treated in §3. The experimental program is common to §§3 and 4 and is discussed in §2.

2. Experimental programme

The experimental programme involved measurements with four types of interactions: a single swept shock wave, the intersection of two swept shock waves, a single weak swept expansion wave, and the intersection of a swept shock wave and expansion wave. Surface pressure measurements were taken in the first two cases while surface flow patterns were recorded for all cases. The test conditions are summarized below:

Mach Number, $M_\infty = 1.85$.
Stagnation pressure, $P_0 = 3 \times 10^5$ Pa,
Stagnation temperature, $T_0 = 300$ K,
Reynolds number, $Re/\text{mm} = 3.9 \times 10^4$ mm^{-1},
Average boundary-layer thickness, $\delta_{av} = 1.9$ mm,

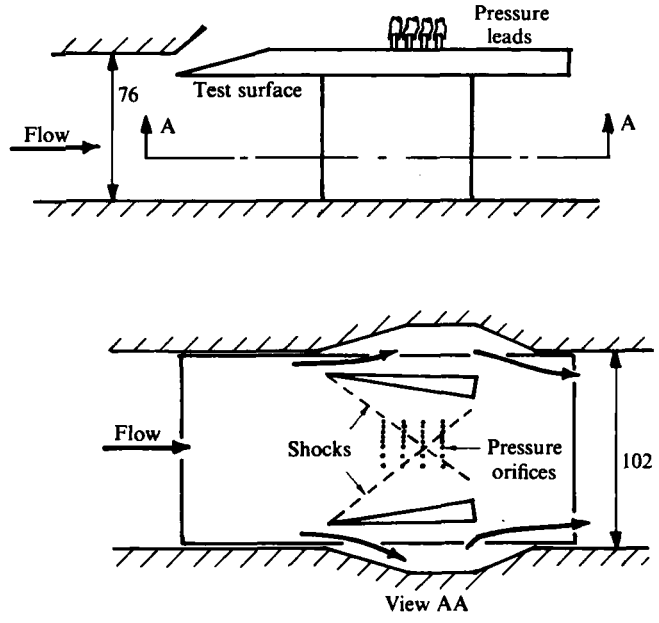

FIGURE 2. The test section (dimensions in mm).

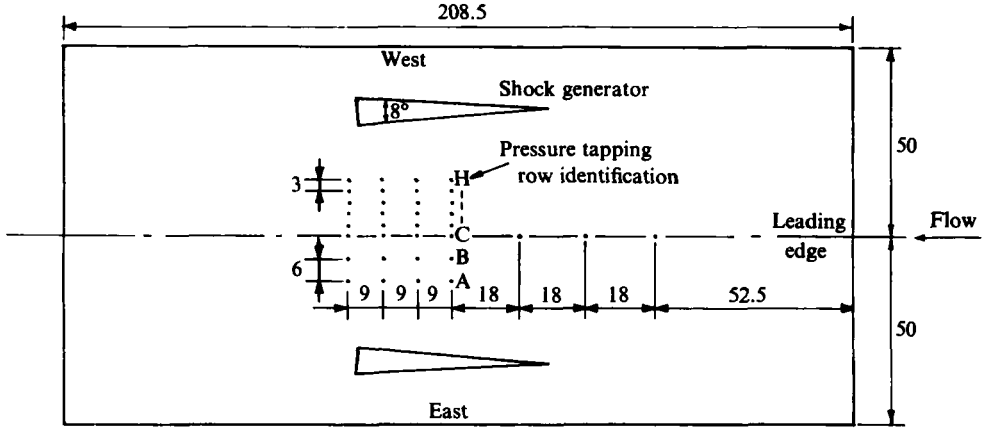

FIGURE 3. The flat-plate test surface (dimensions in mm).

Wedge combinations tested (minus sign indicates expansion):
single 2° to 10°, −3°,
double 2°, 5°; 2°, 7°; 2°, 9°; 3°, 3°; 3°, 5°; 3°, 7°; 5°, 5°; 5°, 7°; −3°, 5°; −3°, 7°.

The experiments were conducted in the University of Queensland supersonic blowdown tunnel, the 76 × 102 mm test section of which is sketched in figure 2 showing the arrangement for the intersecting shock tests. A thin boundary layer was developed for the present experiments using a flat plate to form a test surface as shown in the figure. This test surface, on which the pressure measurements and surface streamline patterns were taken, is sketched in figure 3. The shock and expansion waves which swept across the flat-plate boundary layer were generated by wedges of chord length 50 mm and height 67 mm which were mounted from the

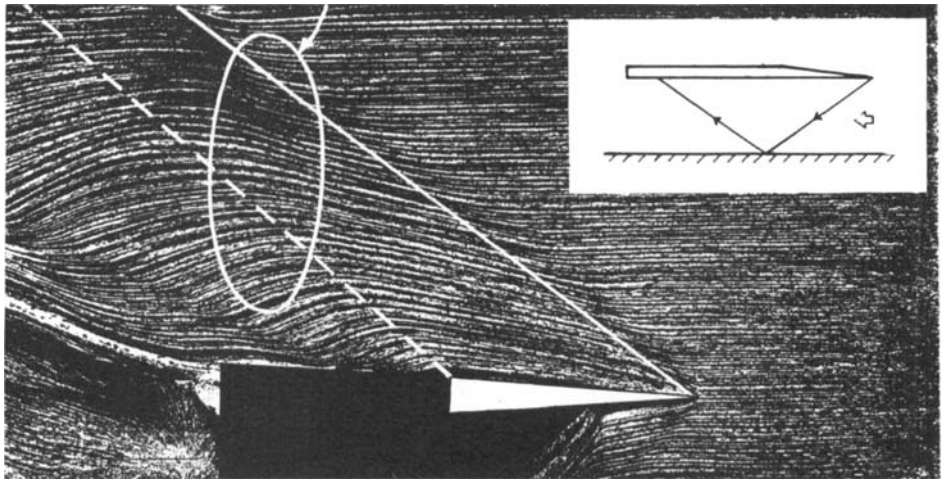

FIGURE 4. Surface streamline pattern, 5° wedge east.

tunnel sidewalls. The wedges were positioned approximately 80 mm from the leading edge of the measuring plate for pressure measurements and approximately 50 mm when surface flow visualizations were recorded. Surface pressures were measured using an array of eight rows of four static pressure holes of 0.5 mm diameter with a 32-channel pressure sensor module. The test surface could be moved relative to the wedges by ± 9 mm. For pressure measurements, with any given experimental configuration, a total of at least seven runs was made with the test surface usually being moved in increments of 3 mm between runs.

The surface streamlines on the flat plate were visualized using the china-film technique. First the surface was covered with a dark blue adhesive tape. A paste made by mixing kaolin with methyl salicylate was then brushed over the taped surface. A 5 s run was sufficient to form the surface pattern as the paste formed surface streamlines and the methyl salicylate began to evaporate. When the plate was removed from the tunnel the remaining 'oil' evaporated leaving the kaolin as white surface streamlines, clearly visible against the blue background. The tape was then removed, attached to cardboard and sprayed to fix the pattern.

A problem in the experiments was associated with the development of the test boundary layer. The sharp leading edge of the measuring plate tended to deflect slightly causing a weak compression then expansion to be generated. This wave pattern reflected from the opposite tunnel wall and then struck the test surface downstream of the array of pressure measuring holes. While the effect of this on the pressure measurements was not significant (since the affected region is downstream of the measurement points), the flow visualizations do show an area of influence where there is extra surface-streamline deflection (see figure 4). Thus the region available for the interpretation of surface-streamline deflections was limited.

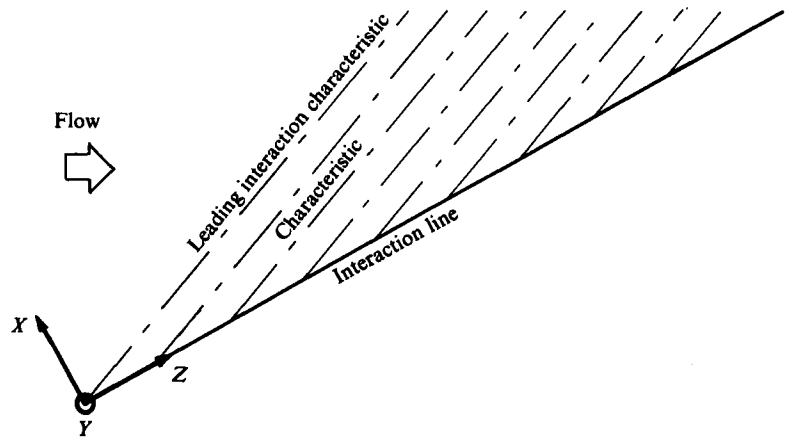

FIGURE 5. Shock/boundary-layer interaction characteristics.

3. The nature and development of a single shock interaction

3.1. *Introduction*

The theoretical analysis of Stalker (1984) indicates the way in which a swept-shock-wave/boundary-layer interaction develops in the spanwise direction. It predicts that perturbations to flow quantities along the interaction line† are propagated upstream of this line with exponential decay along a series of parallel shock/boundary-layer interaction characteristics (see figure 5). This leads to the conclusion that if properties are constant along the interaction line, then the flow between this line and the leading interaction characteristic will take a cylindrically symmetric (CS) form. Further upstream of the leading characteristics the theory suggests that properties will take their undisturbed values implying a sudden jump in flow properties occurs across the leading characteristic. These sudden jumps will in practice be 'smoothed out' on either side of this characteristic since the boundary layer will not accept infinite gradients in properties. If the theory took into account the flow in the region close to the shock generator, it is expected that properties upstream of the leading characteristic would be influenced by the spanwise propagation of the disturbances along a further set of characteristics. This possibility is investigated in § 3.2.

Taking the distribution of the deflection angle of the boundary-layer streamlines normal to the surface, $\eta(= v/U$, where v is the y velocity component and U is the undisturbed x velocity component), to be CS between the shock wave and the leading interaction characteristic, Stalker used linearized supersonic flow theory to determine the associated mainstream pressure distribution and found that this was only approximately CS, slowly approaching an asymptotic value away from the shock generator. In this paper it is suggested that there is in fact a more rapid increase in boundary-layer thickness close to the shock generator while the associated mainstream pressure drops in that region and the surface pressure is approximately constant at the shock position.

Away from the shock generator all properties approach a true CS form and the interaction is termed fully developed. These observations are consistent with the

† The interaction line is nominally the inviscid shock position; however as indicated later this line may lie upstream of the shock.

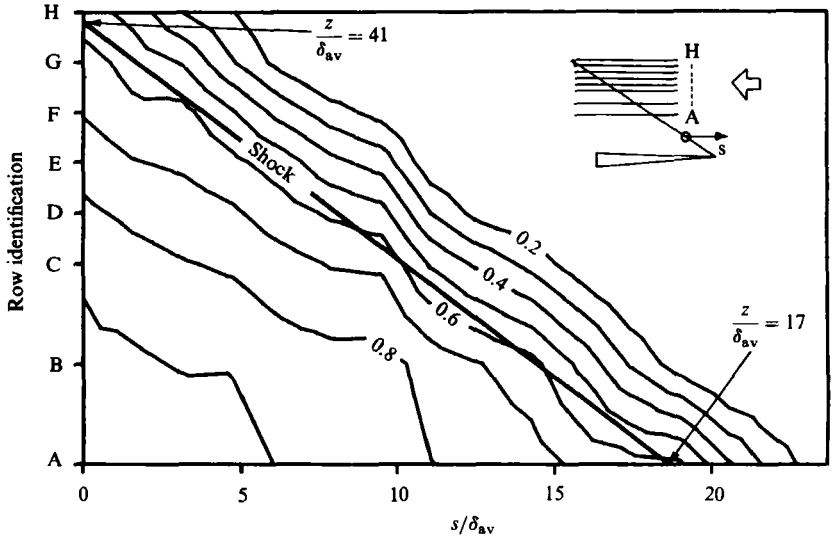

FIGURE 6. Surface isobars far from the wedge, 5° wedge east (row A closest to the wedge). Contours of $(p\text{-}p_0)/\Delta p$ (Δp is the pressure rise across the shock).

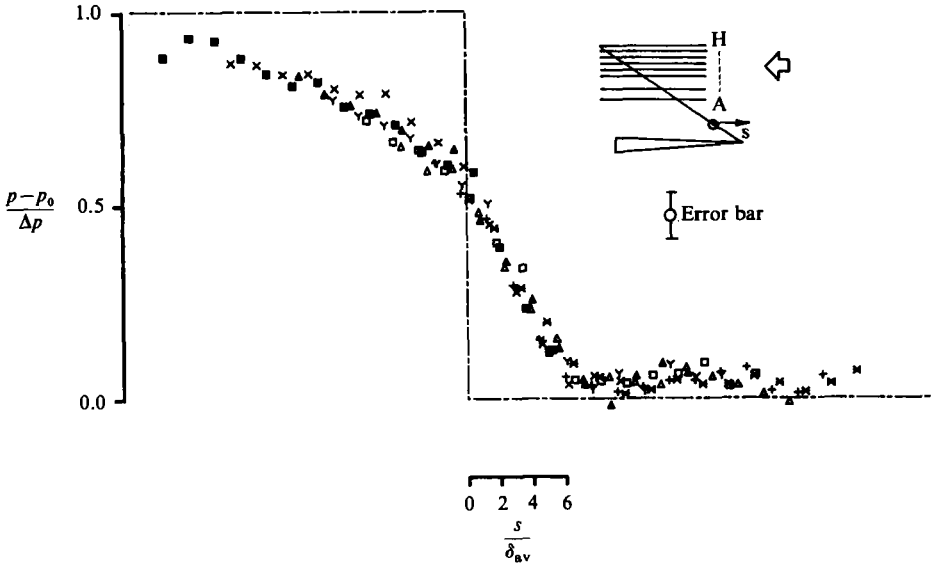

FIGURE 7. Surface pressures plotted relative to the shock position 5° wedge east. ■, X, ▲, Y, □, △, +, *, measurements at rows A to H respectively (row A closest to the wedge).

characteristics analysis and available experimental results as discussed in §§ 3.2 and 3.3.

3.2. *Testing the characteristics model*

As mentioned in the previous section, the flow should develop a CS form well away from the shock generator. Surface pressures were measured in the region where the characteristics analysis predicts that the flow will be nearly fully developed and thus close to the CS condition. For surface pressures this was checked by two methods. First, surface isobars were plotted. For a CS flow field isobars should be parallel to

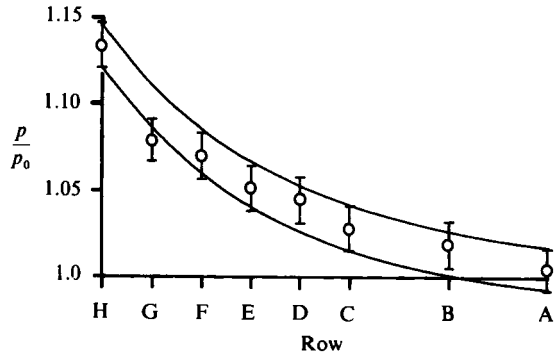

FIGURE 8. Pressure decay along the leading characteristics, 5° wedge west. ◊, measured pressure and error; solid lines indicate the predicted exponential decay from the pressure measured at row H (row H closest to the wedge).

the shock wave. This is found to be the case away from the shock generator and a sample isobar pattern in this region for the wedge at an angle of 5° is presented in figure 6. Making some allowance for experimental errors (see figure 7) the isobars are seen to be essentially parallel to the interaction line. The second way to present the data in order to check for cylindrical symmetry involves plotting the surface pressures along each of the measuring lines relative to the position of the shock on each of those lines. A cylindrically symmetric pattern will result in all distributions falling on a single curve. Such a curve is shown in figure 7. Away from the shock generator the surface flow patterns also indicate that the flow is approaching a CS form.

The surface pressures plotted in figure 7 take a similar form to those obtained in experiments by various other researchers with both two- and three-dimensional configurations (e.g. Gadd 1961; McCabe 1966) as well as in theoretical analyses (e.g. Inger & Mason 1976; Messiter 1980).

The pressure does not decay exponentially upstream starting at the inviscid shock position, but rather the true exponentially decaying region starts a small distance upstream of the shock. Since Stalker's (1984) analysis has been developed for the region where disturbances are decaying exponentially upstream, an interaction line for the analysis would necessarily lie slightly upstream of the shock location.

In order to further test if the characteristics analysis is consistent with the experimental observations, a series of tests was performed to measure surface pressure distributions along streamwise rows close to the shock generator in the region where the interaction is first developing. A check on the characteristics model can be made by measuring the decay along a characteristic to see if it is exponential and if the rate agrees with the decay rate in the region where the interaction is approaching the fully developed state. This check was performed by first measuring the decay rate in the region where surface pressures take a CS form. The component of this decay rate in the calculated direction of the characteristics was then determined. Starting at the streamwise line closest to the shock generator at which pressures were measured, pressures were predicted at other streamwise lines by decaying the pressure at the first line along a characteristic at the rate determined. As shown in figure 8, the measured pressures agree with the decayed results to within the accuracy of the experiment.

The form of the experimental results indicates that disturbances upstream of the leading interaction characteristic are propagated in a spanwise direction along a

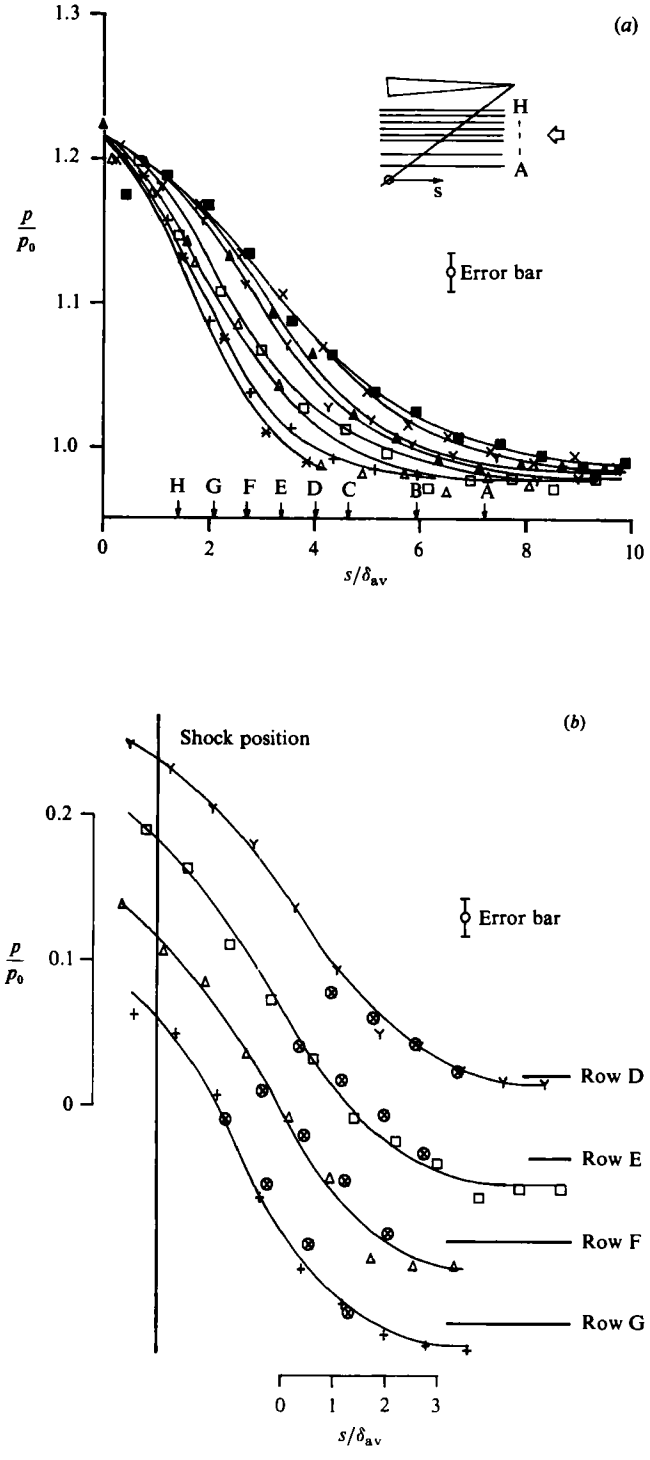

FIGURE 9. Surface pressure close to the wedge, 5° wedge west. (*a*) Distributions on each row. (*b*) Measured distributions showing comparison with pressures decayed from row H along characteristics. (row H closest to the wedge). ↓ indicates the position of the leading characteristic; ⊗, pressures decayed from row H; ■, X, ▲, Y, □, △, +, * measurements at rows A to H respectively.

further set of parallel characteristics. In fact it is suggested that all effects upstream of the interaction line are the result of spanwise propagation of disturbances except in a small region close to the shock generator. What happens in that region cannot at present be explained in terms of the characteristics analysis. The surface pressures measured just outside that region are plotted relative to the shock position in figure 9(*a*). The position of the leading interaction characteristic on each of the lines is also indicated. In terms of the model being examined here, one would expect to see the pressure distributions merge towards a single curve some distance downstream of the location of the leading characteristic on each line. Taking into account the scatter due to experimental errors this trend can be seen in the distributions. The pressures on rows E–H do not merge ahead of the shock because the leading characteristic cuts these lines quite close to the shock. The suggestion that disturbances upstream of the leading interaction characteristic are propagated along parallel characteristics was also examined using this surface pressure data. Starting with the pressures measured along the line closest to the shock generator, pressures were decayed along characteristics using the decay rate as determined above. The predicted pressures along each of the measuring lines were then compared with the measured distributions. The sample results presented in figure 9(*b*) indicate that pressures in the region where the interaction is developing may be explained in terms of spanwise propagation of disturbances along characteristics.

3.3. *A model for the interaction*

As mentioned in § 3.1, a model of the interaction involving a CS distribution for η leads to the distribution of pressures at the edge of the boundary layer, p_δ, taking a non-CS form. If instead a CS form is taken for the p_δ distribution, a non-CS form will result for the η-distribution. Which of these possibilities occurs in practice, or is there some compromise between the two? This section deals with this question and its implications. The answer proposed is that there is indeed a form of compromise.

Experimental evidence suggests a model involving more rapid boundary-layer thickening close to the shock generator. The surface flow visualizations of the present experiments as well as that of McCabe (1966) indicate that there is more deflection of the surface streamlines close to the shock generator than there is further away. (This is separate from the extra deflections caused by the partial bluntness of the wedge's leading edge.) Results from experiments of Stalker (1958), in which surface pressures were measured for a glancing shock, indicated that for a limited range of wedge deflection angles the pressure distributions took the characteristic separated form close to the shock generator, while the distributions showed an unseparated form further away from the shock generator. This again is consistent with more rapid boundary-layer thickening in the region where the interaction is first developing, as greater cross-flow upstream separates the flow, yet where the interaction is fully developed reduced cross-flow leaves the flow attached.

The model of the interaction proposed here achieves greater boundary-layer edge-deflection angles in the region where the interaction starts to develop by superposition of a series of CS η distributions to produce a resulting distribution in which the edge-deflection angle increases towards the shock generator. This is possible because the equations which describe the flow field are linear. This can be seen by writing the three-dimensional equations for the two boundary-layer decks (Stalker 1960). In vector operator form they appear as

$$(\mathbf{U}(y)\cdot\nabla)\,\mathbf{u}+v\,\mathbf{U}'(y) = -\rho(y)^{-1}\nabla p, \tag{1a}$$

$$\nabla\cdot\mathbf{u} = -(\gamma p_0)^{-1}\,\mathbf{U}(y)\cdot\nabla p, \tag{1b}$$

for the inviscid middle deck, and

$$(\mathbf{U}(y)\cdot\nabla)\mathbf{u}+v\mathbf{U}'(y)=-\rho_s^{-1}\nabla p+\nu_s\nabla^2\mathbf{u}, \tag{1c}$$

$$\nabla\cdot\mathbf{u}=0, \tag{1d}$$

for the viscous, incompressible, inner deck. Here the Cartesian coordinates x, y, z are chosen with y normal to the surface, as shown in figure 5. The vector $\mathbf{U}(y)=[U_x(y),\ 0,\ U_z(y)]$ represents the velocity distribution in the undisturbed boundary layer upstream of the interaction $\rho(y)$ and p_0 are the undisturbed density and pressure, ρ_s and ν_s are the undisturbed density and kinematic viscosity at the surface, and the vector $\mathbf{u}=(u,v,w)$ and the scalar p are the small disturbances in velocity and pressure. γ is the ratio of specific heats. Clearly these equations are linear in $\mathbf{u}$ and p. Thus, the superposition of CS solutions, which leads to extra vertical boundary-layer deflections, is permissible. It will lead to extra lateral cross-flow and thus to greater surface-streamline deflection close to the shock generator.

To predict the increased surface-streamline deflection, the measured surface-pressure distribution can be used with allowance for pressure change across the boundary layer. This yields the pressure at the edge of the boundary layer and a series of CS η-solutions can then be superposed to produce this pressure distribution.

The pressure at the edge of the boundary layer can be found relative to the wall pressure from simple extensions to the theory developed by Stalker (1984). It can be shown that

$$p'_\delta=p'_w-\left(\frac{\partial\eta}{\partial x}\right)_\delta\int_0^\delta M_x(y)^2\,dy, \tag{2}$$

where $p'=(p-p_0)/(\gamma p_0)$, p is the static pressure, p_0 the undisturbed value, γ is the ratio of specific heats, $M_x(y)$ is the profile of the component normal to the shock of the undisturbed Mach number, and the subscripts δ and w refer to values at the edge of the boundary layer and at the wall respectively. Then $(\partial\eta/\partial x)_\delta$ is found from

$$\left(\frac{\partial\eta}{\partial x}\right)_\delta=p'_\delta\left\{M_{x_\delta}^4\beta^{-1}\int_0^\delta(M_x(y)^2-1)\,dy\right\}^{-1}, \tag{3}$$

where $\beta=(M_{x_\delta}{}^2-1)^{\frac{1}{2}}$.

Turning now to the present series of experiments, surface-pressure measurements indicate that, in the vicinity of the shock wave, isobars run approximately parallel to the shock, even in the interaction development region (see figures 6 and 10). This suggests that the surface pressures will be approximately constant along a line parallel to the shock and downstream of the influence of the smearing of the pressure increase at the leading interaction characteristic. For this reason p'_w in (2) is taken to have a CS distribution.

Using the Mach-number profile $M(y)=M_\infty(y/\delta)^n$ with $n=0.25$, distributions of η and p'_δ along a line upstream of and parallel to the shock wave have been determined for constant p'_w. For the 5° wedge these distributions are shown in figure 11. In this figure, Z has been normalized using κ^{-1}, the distance normal to the shock over which the pressure decreases by a factor of e. These results indicate that p'_δ drops towards the shock generator ($Z=0$) while η increases. Far removed from the shock generator the properties approach a constant value and the flow field is cylindrically symmetric. These distributions have been obtained for a CS p'_w distribution. However, η and p'_δ distributions could be found for any given surface pressure distribution by the same technique.

It might be noted that this approach leads to an inconsistency in that the pressure

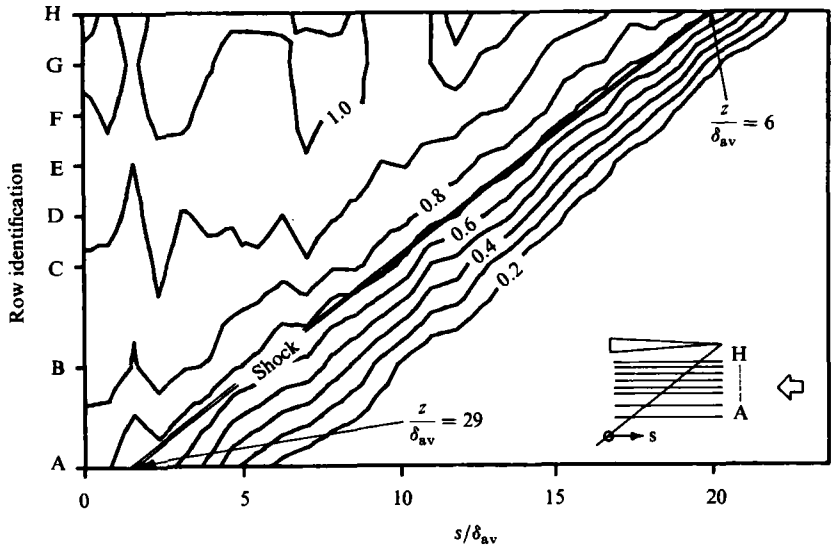

FIGURE 10. Surface isobars close to the wedge, 5° wedge west (row H closest to the wedge). Contours of $(p-p_o/\Delta p)$.

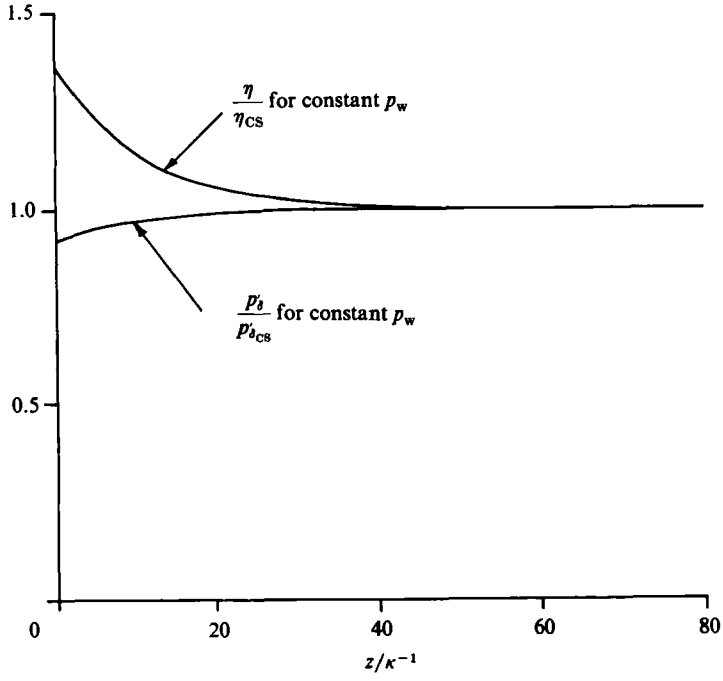

FIGURE 11. η and p_δ distributions along a line upstream of and parallel to the interaction line. Curves for 5° wedge.

variation in the X-direction, associated with the p'_δ in figure 11, will only be an approximation to that required to produce the associated distribution of η. That is, there is a mismatch between the boundary layer and mainstream solutions. It is assumed here that the adjustments to the boundary-layer flow which are required to eliminate this mismatch can be neglected.

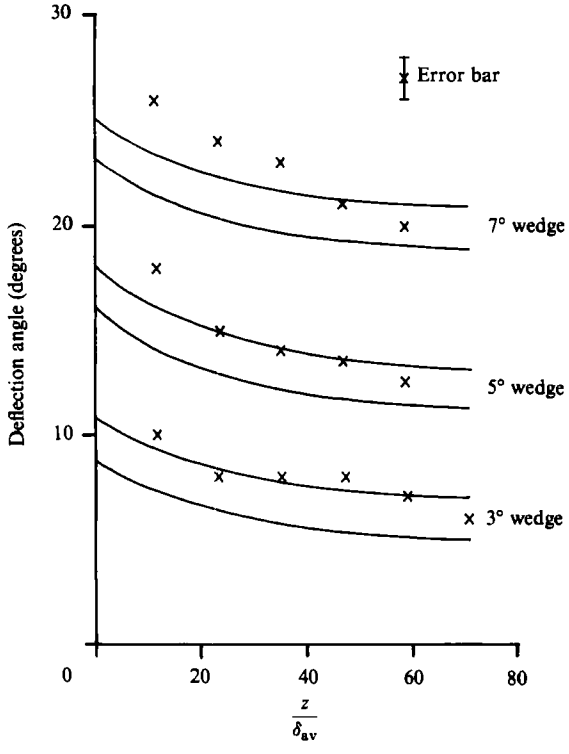

FIGURE 12. Surface streamline deflection angles at the shock position. ×, measured values; solid lines indicate angles predicted from the measurements at the extreme Z location.

As noted above, the more rapid boundary-layer thickening near the leading edge of the wedge was obtained by superposition of a series of linear CS solutions. Since a perturbation analysis has been applied, the increase in surface streamline deflection angle in the interaction development region will be proportional to the excess η in that region. From the surface flow visualizations, angles of streamline deflection were measured along a number of lines parallel to the tunnel walls at different distances from the wedge. The angle at the shock position was then plotted against the distance from the wedge. Starting from the deflection angle measured at the most extreme Z-position, the increase in deflection angles at the other positions according to the calculated edge-deflection distribution was determined. The results for the 3°, 5° and 7° wedge angles are presented in figure 12.

The curves show the same trend although discrepancies are larger than can be explained by experimental and measurement inaccuracies. This may be due to the inaccuracy of the small perturbation approximation at large surface flow deflection angles. The angles at the first measuring line are probably pushed high because they remain in the region of influence of the partial bluntness of the leading edge of the wedge. It can be seen that there is relatively little change in deflection angle from the shock generator to where the interaction is fully developed.

It may be noted (e.g. figure 4) that the surface flow-visualization patterns indicate that the region downstream of the shock close to the wedge may have significantly different properties from the remainder of the flow field. A surface streamline approaching the nose of the wedge will be deflected through a greater angle than the angle of the wedge itself. This leaves a region between that streamline and the wedge

where the flow must take a different character. Initial experiments indicate that, for the non-separated flow fields studied here, the flow in this region does not come from the face of the wedge onto the plate. In this region there is significant streamline divergence, particularly as the shock strength increases (see figures 4 and 17). This will lead to a thinning of the boundary layer and subsequent increases in heat transfer rates and skin friction magnitudes in that region. In their experiments with comparatively stronger shocks Kubota & Stollery (1982) suggested a vortex formed in this region as fluid flowed from the wedge onto the face of the plate. The present experiments suggest that for weak shocks, downstream increases in heat transfer and skin friction can take place without vortex formation.

The model of more rapid boundary-layer edge deflection in the region where the interaction is first developing is consistent with the characteristics analysis and available experimental observations. More detailed flow measurements in the boundary layer would be desirable to further test the applicability of the proposed model for swept-shock-wave/boundary-layer interactions.

4. Intersecting oblique shock and expansion waves

4.1. *Introduction*

As already noted, the intersecting-shock situation provides an opportunity for further testing of a feature of the triple-deck small disturbance model – namely that a superposition principle is expected to apply. Equations (1*a–d*) which are linear in velocity and pressure terms indicate that solutions to two interaction problems can be added to satisfy the middle- and inner-deck equations for a third. The boundary condition at the surface, $v = 0$, is also satisfied. If the linearized equations of supersonic flow apply in the outer deck, or mainstream, the solutions there can also be added. The complete disturbance flow fields therefore may be combined linearly, or superposed, in order to produce a third flow field. It may be objected that, for the intersecting shock waves involved here, the flow normal to the shock is transonic, and so nonlinear flow regions are present in the outer deck. However, Inger & Mason (1976) have shown that two-dimensional interactions with weak normal shocks can be treated with linearized supersonic and subsonic mainstreams respectively upstream and downstream of the shock waves. It is plausible to assume that the same approximation will be equally effective here, so that linearized flow prevails in the outer deck, and the interaction fields of the two intersecting shocks may be superposed to produce the resultant interaction field.

The superposition hypothesis is to be tested here for surface-pressure distributions as well as surface streamline directions. The linearization of the boundary-layer equations implies that disturbances to flow quantities are much smaller in magnitude than the corresponding undisturbed quantity. Thus, in the case of surface pressures, the perturbations for two single-shock/boundary-layer interactions can simply be added to obtain the pressure perturbations for the colliding shock/boundary-layer interaction. The surface streamline directions give the direction of shear stress at the surface. Thus if small perturbations are assumed, the shear stress changes little in magnitude across a single, weak shock or expansion. Then, if perturbations are again small through the second shock or expansion, the resulting shear stress direction can be obtained by adding the angle of deflection through each of the single interactions.

It should be noted that superposition is only an approximation even for the mainstream. Superposition of two single-shock results will underestimate the total pressure increase achieved downstream of a double-shock interaction. This is because

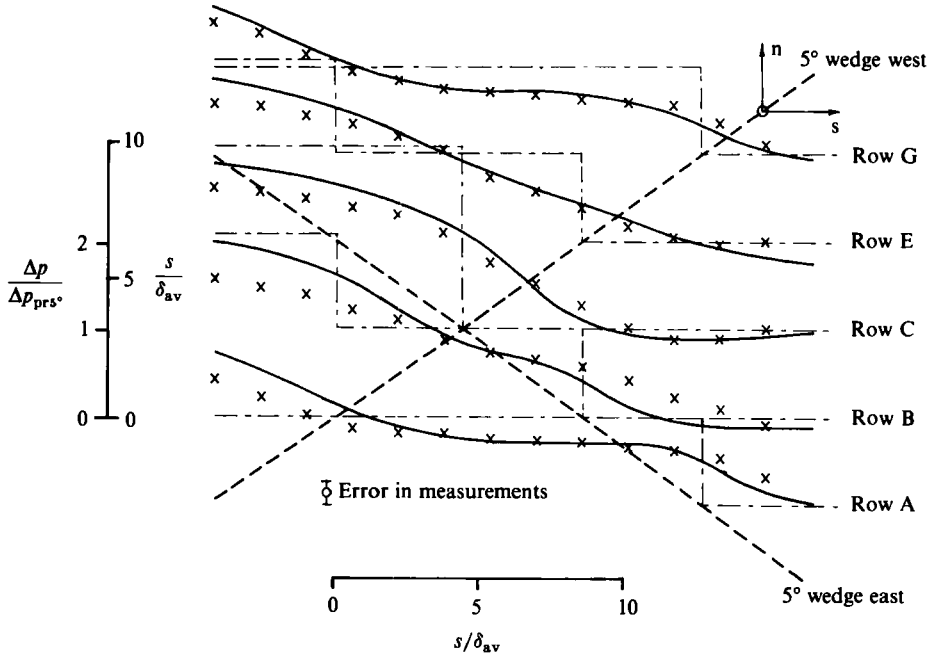

FIGURE 13. Surface pressure distributions at the shock intersection, $2 \times 5°$ wedges. Solid lines indicate measured distributions; ×, superposition results; chained lines indicate inviscid distributions; dashed lines indicate surface positions of shocks.

the reduction in Mach number across the first shock results in a larger pressure increase across the second shock and thus a higher pressure downstream of the shock intersection. Subsequently, pressures obtained through superposition are expected to be slightly less than measured values for a double-shock interaction near and downstream of the second shock.

The experiments reported here test the superposition principle through measurements on the interaction at the intersection of glancing shocks produced by an opposing pair of wedges in a supersonic tunnel. Tests are also reported of the intersection of a glancing shock wave with a weak glancing expansion wave. In experiments on linear theories in aerodynamics it has been usual in the past to test them beyond their strict range of application. The same principle is followed here and although the small-disturbance theory is intended to apply to interactions which are well removed from separation, the tests are conducted up to shock strengths approaching the separation value. (Incipient separation occurs at wedge angles between 9° and 10°.)

4.2. *Results*

Considering first colliding shocks of equal strength, the pressure distribution measured at the surface of the plate near the intersection of shock waves generated by two wedges, each at an angle of 5°, is shown in figure 13. In plotting these results, the pressure rises are normalized with respect to the inviscid pressure rise achieved across the first shock wave. Distances are normalized with δ_{av}. The pressures are plotted in a semi-three-dimensional form with the vertical scale representing both spanwise plate length and normalized pressures, the zero pressure for each streamwise line being the surface position of that line. The pressure distributions along five

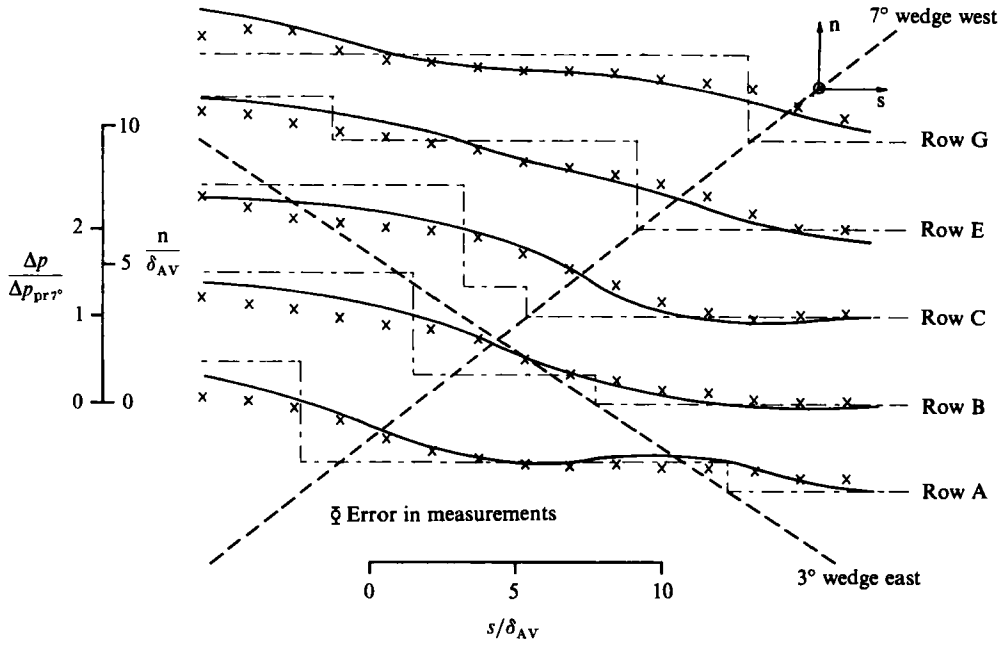

FIGURE 14. Surface pressure distributions at the shock intersection. 3° wedge east and 7° wedge west. Solid lines indicate measured distributions; ×, superposition results; chained lines indicate inviscid distributions; dashed lines indicate surface positions of shocks.

streamwise rows are shown. The inviscid-surface-shock position is shown by the dashed line. The inviscid pressure distributions are indicated by a chained line. Also shown in the figure are the results of superposition of two measured single-shock pressure distributions. The results compare well and the expected mismatch is evident downstream of the intersection due to the fact that superposition does not predict the overall pressure rise as discussed in § 4.1.

Superposition will give an indication of the extent of the influence of the shock intersection region. The downstream shock will only affect the upstream one over a distance of the upstream influence found in a single-shock interaction. Applying this idea, the lateral effect of the intersection can be predicted.

Turning to shocks of unequal strength, the measured surface-pressure distribution obtained in the region of intersection of a shock wave generated by a 3° wedge and that generated by a 7° wedge is presented in figure 14. Shown also in this figure is the pressure distribution obtained through superposition of the two single-shock results. Again measured and superposed results compare well. The surface streamline pattern for the symmetric colliding shock case for wedge angles of 5° is given in figure 15 and that for the single 5° wedge in figure 5. Note that the streamline through the centre of the interaction deflects only minimally. The pattern is not perfectly symmetric because the wedges are not exactly the same and the flow uniformity of the tunnel is not perfect. Angles of deflection were measured along three streamwise lines; one coincident with the intersection of the inviscid shock positions and the other two lines $5\delta_{av}$ either side of the centreline. Measurements were also made for the two single-shock surface flow patterns along lines at the same positions relative to the wedges. The single-wedge results were superposed in the manner described in § 4.1 and are compared in figure 16 with the measured double-shock results. The

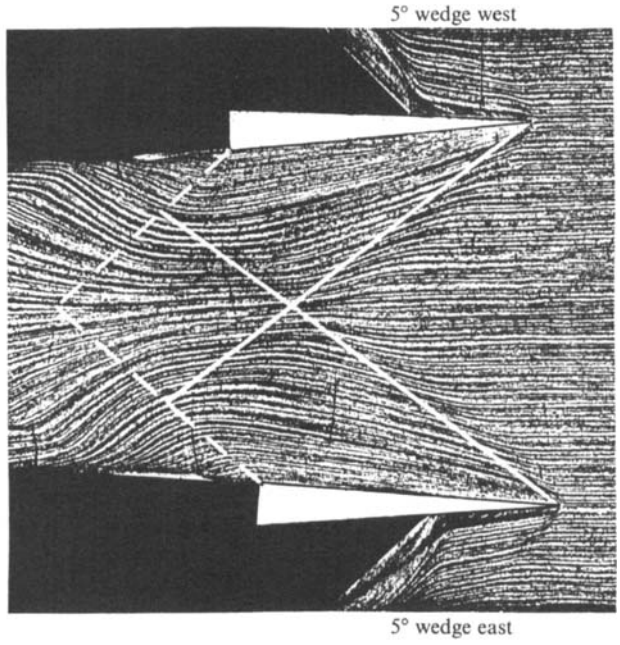

FIGURE 15. Surface streamline pattern, $2 \times 5°$ wedges.

deflections are plotted in a manner similar to the semi-three-dimensional pressure plots. Here the vertical scale represents both spanwise plate length and deflection angle with the zero of angle for each line being the surface position of the line. Positive angular deflection is taken as being towards the lower (eastern) wedge. These results indicate a high correlation between the superposed and measured results. A further check is made on the validity of superposition of surface streamline direction with the non-symmetric colliding shock interaction for shocks generated by wedges at angles of 3° and 7°. The double-shock surface streamline pattern is shown in figure 17. Measured angles for this double-shock case are compared with superposition of the single-shock results along three streamwise lines in figure 18. While results again compare well, the results obtained using superposition indicate slightly smaller angular deflections than measured values for the double-shock interaction. Applying superposition to the 7°, 3° interaction may be extending the concept beyond its strict range of applicability. However, as mentioned in § 4.1, linear theories are often used in such a manner with good results. The agreement between superposed and measured surface pressures and streamlines obtained here encourages the application of superposition for shocks that are not weak.

The results that have been obtained for superposition of surface streamline deflection angles indicate that the deflection angle reduces relative to the undisturbed flow direction on passing through the second shock wave. In the past, surface streamline patterns have often been used to determine whether three-dimensional flow separation has occurred (e.g. Lighthill 1963; McCabe 1966; Oskam 1976). Taking that a reduction in streamline deflection angle indicates a step away from incipient separation, the present results for shock/shock intersections suggest that the flow will be removed from separation on passing through the second shock. This leads to the question of what will happen if a shock wave which has significantly deflected surface streamlines encounters an expansion wave which tends to deflect the flow in

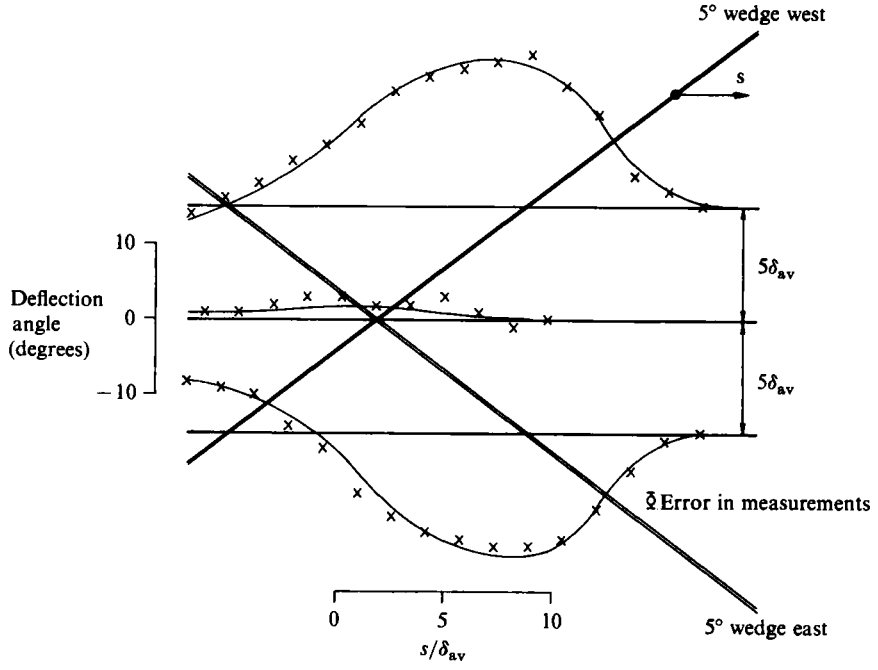

FIGURE 16. Surface streamline deflecting angles along three streamwise lines, $2 \times 5°$ wedges. Solid lines indicate measured distributions; ×, superposed results; double lines indicate surface positions of shocks.

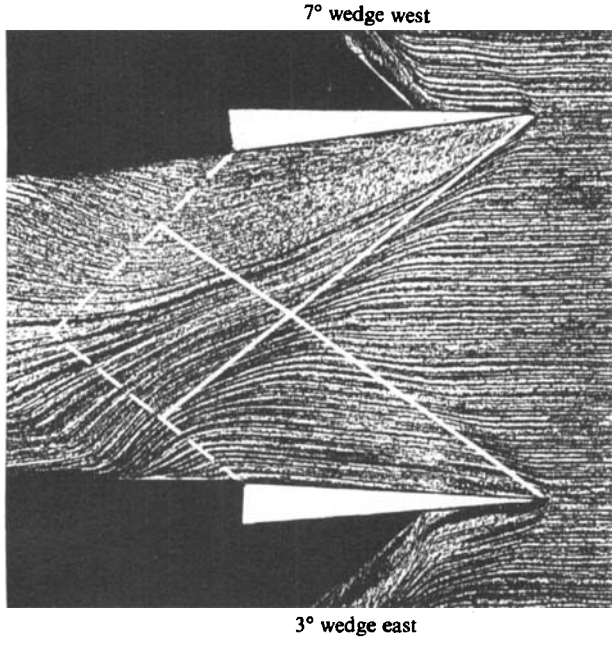

FIGURE 17. Surface streamline pattern, 3° wedge east and 7° wedge west.

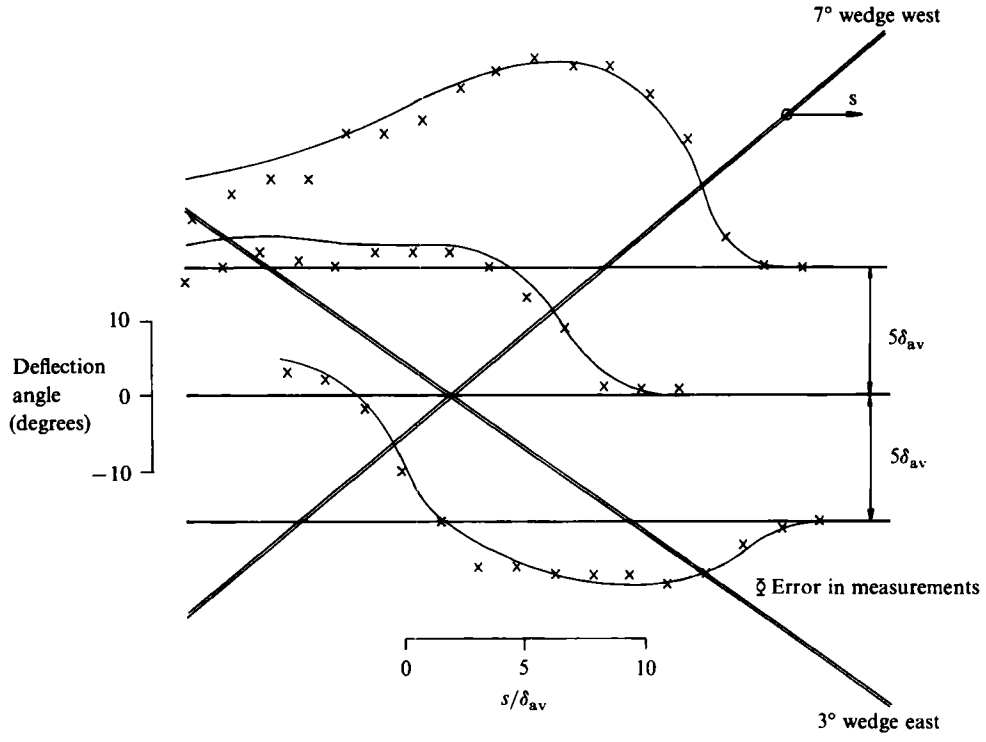

FIGURE 18. Surface streamline deflection angles along three streamwise lines, 3° wedge east and 7° wedge west. Solid lines indicate measured distributions; ×, superposed results; double lines indicate surface positions of shocks.

the same direction. The superposition principle which has been shown to apply in the weak shock/shock intersection suggests that a shock/expansion intersection will lead to increased deflection of surface streamlines downstream of the intersection. Will, therefore, a shock wave that is not quite strong enough to cause boundary-layer separation, on intersection with an expansion wave, lead to separation? In an attempt to answer this question a preliminary series of tests, involving surface flow visualizations of the intersection of a glancing shock wave with a weak glancing expansion wave, was completed.

Experiments involving a shock/expansion intersection were difficult to perform in the small wind tunnel used in the present experimental programme because of problems involving choking of the flow. However results were obtained for the intersection between the shock generated by a wedge at angles of 5° and 7° and an expansion caused by a wedge at an angle of −3°. The surface flow pattern obtained for the interaction of the expansion wave with the boundary layer is shown in figure 19(*a*). Since the inner face of the wedge causing the expansion is at an angle of −3° to the oncoming stream and the included angle of the wedge is 8°, the outer face of the wedge is at an angle of 11° to the flow. This leads to strong compression of the flow behind the wedge. (If the compression is too great, the flow in this region becomes choked and a certain amount of the flow spills over the front of the wedge. This effect is evident to a small extent in the −3° wedge flow pattern with a slight compression before the expansion.) The resulting pressure difference across the wedge has led to some seepage through the wedge-plate interface. The surface flow pattern

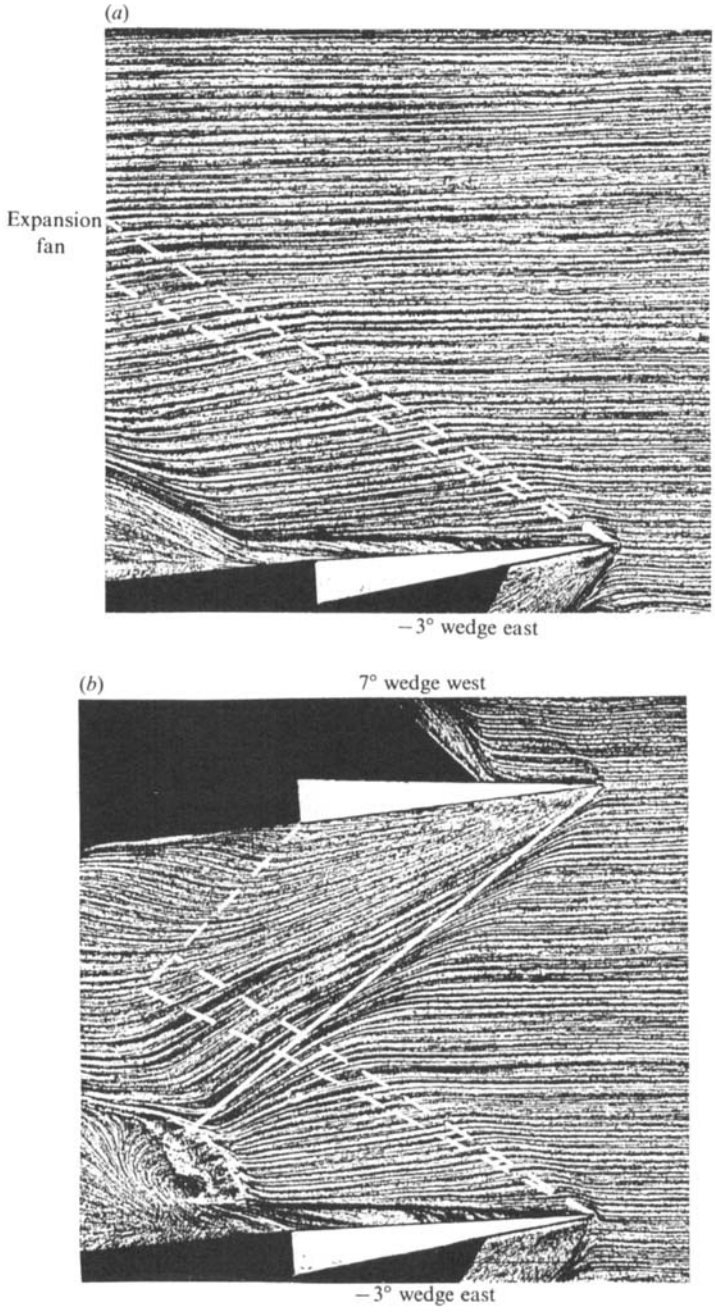

FIGURE 19. Surface streamline patterns. (*a*) −3° wedge east; (*b*) −3° wedge east and 7° wedge west.

for the 7°, −3° intersection is given in figure 19(*b*). This pattern does indicate an increase in deflection angle after the flow passes through the shock then the expansion wave. The end of the wedge interferes with the flow field before the full impact of the interaction can be determined. Measurements of deflection angles along three streamwise lines have been made; one line coincident with the intersection of

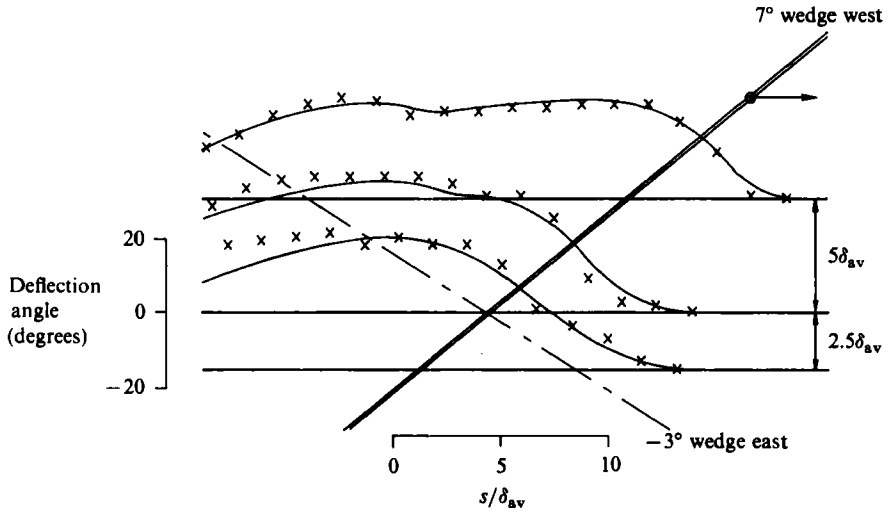

FIGURE 20. Surface streamline deflection angles along three streamwise lines, −3° wedge east and 7° wedge west. The chained line indicates the surface position of the leading edge of the expansion fan. Solid lines indicate measured distributions; ×, superposed results; double line indicates surface position of shock.

the inviscid shock and expansion waves, one line $5\delta_{av}$ toward the 7° wedge and the other line $2.5\delta_{av}$ towards the −3° wedge. Results are shown for these measurements and for the superposition of the results for the two single interactions in figure 20. The superposed results again show close agreement with the measured angles.

Although the surface-streamline deflection angle increases through the expansion in line with expectations from consideration of superposition, the question of whether this will lead to flow separation has not been answered. For the 7°, −3° intersection both superposed and measured deflection angles suggest that the surface flow does not turn through an angle as great as that of the shock (maximum deflection angles of 34° measured and 36° superposed compared with a shock angle of 40°). However, superposition does suggest that the flow in the case of a 9°, −3° intersection will turn the surface streamlines downstream of the intersection through an angle greater than that of the shock. A flow visualization of this configuration was attempted but the constriction to the flow behind the expansion wedge led to further leakage of the flow around the leading edge of the wedge which disrupted the flow field. The short run before the recompression downstream of the end of the wedge also limited the region of interest. The general form of the surface streamline pattern predicted by superposition for the case where the streamlines downstream of the intersection are turned through an angle greater than the shock angle is shown in figure 21. Downstream of the expansion, but just before the shock wave, a line can be identified which runs parallel to the shock and to which the streamlines converge. The surface streamlines behind the shock downstream of the intersection are deflected such that they approach the shock and also eventually approach the convergence line asymptotically. However, if convergence of streamlines upstream of the shock does occur and this leads to separation, the character of the flow downstream will be changed and the streamline pattern there indicated by superposition will not be obtained.

The question of criteria for three-dimensional separation in shock/boundary-layer interactions has again been raised. For a single swept-shock/boundary-layer inter-

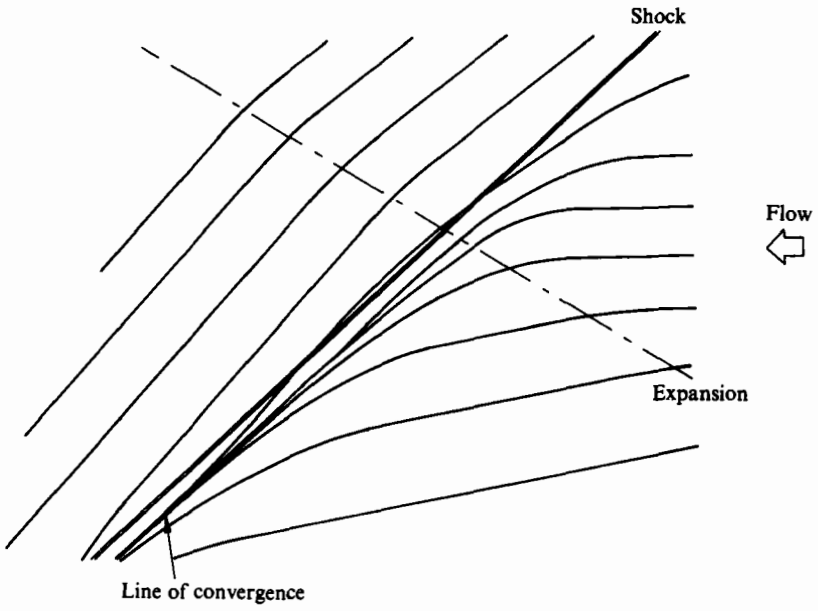

FIGURE 21. Surface streamline pattern predicted by superposition for a shock expansion intersection.

action, Korkegi (1973) suggests incipient separation will occur when the pressure ratio across the shock, p/p_0, reaches 1.5. The present experimental results indicate that while the total pressure rise achieved in the shock/shock interaction will be relatively large, the disturbance to the boundary-layer flow is reduced. In contrast, the shock/expansion intersections produce less overall pressure rise, but disturbance to the boundary-layer flow is significant. Which agency then is the most important in provoking flow separation, a strong, adverse pressure gradient or major disturbances to the structure of the boundary-layer flow? If severe twisting of the boundary layer can induce separation, then an expansion in the presence of a shock wave may disrupt the character of the flow in a region in which one may initially expect wholly attached flow.

5. Conclusions

Detailed surface pressure measurements of the present investigation into swept-shock-wave/boundary-layer interactions are found to be consistent with the characteristics analysis of Stalker (1984). Perturbations to the undisturbed upstream values of quantities are propagated with exponential decay along a series of parallel characteristics which lie upstream of the interaction line. While the characteristics analysis strictly only applies between the interaction line and the leading interaction characteristic, results indicate that, apart from a small region close to the shock generator, the idea of parallel characteristics may explain the flow in the complete region upstream of the interaction line.

A model of the interaction involving more rapid thickening of the boundary layer upstream of the shock wave, close to the wedge, has been presented. This model explains the trend of extra surface-streamline deflection there as evidenced in the surface flow visualizations. However this effect typically leads to only a small

increase in deflection angle at the shock position near the wedge. In contrast to essentially parallel surface streamlines in the majority of the flow field, the streamlines diverge in the region close to the wedge but just downstream of the shock. It is expected that this streamline divergence will lead to thinning of the boundary layer and subsequent increases in heat transfer rates and skin friction magnitudes in that region.

The characteristics model shows that a linear theory can be used to explain this swept three-dimensional interaction. A consequence of this linearity is that superposition of the solutions obtained for two single-shock interactions can be added to give the solution for the case of intersecting interactions. For surface-pressure and surface-streamline distributions this has been shown to be valid for the intersection of two shock waves in the presence of a turbulent boundary layer. Thus, given a method of obtaining these distributions for the single-shock cases, be it through an analytical or numerical model or by direct measurement, the surface pressures and streamlines for a weak shock/shock intersection can be predicted.

The surface streamline patterns for the shock/shock intersections indicate that the streamline deflection angles are reduced on passing through the intersection. Thus the twisting of the boundary layer is decreased. Assuming that greater surface streamline deflection indicates that the flow is closer to separation, the boundary layer is moved away from the separation condition on intersection with a second shock. Therefore, a given overall pressure rise can be achieved with intersecting shocks with less likelihood of separation than the same pressure rise achieved with a single shock.

Superposition of surface streamline deflections has been shown also to be valid for the intersection of a shock and an expansion wave. This interaction results in greater deflection of surface streamlines downstream of the intersection and thus the boundary-layer twisting is increased. This introduces the possibility that an attached boundary layer will separate downstream of the intersection even though the overall pressure rise is reduced.

This programme of work could not have been completed in the time available without the generous assistance of the Workshop Staff, in particular Mr V. W. Mercer and Mr D. R. Sussmilch. One of us (J. L. S.) was in receipt of a Visiting Professorship from the University of Queensland during part of the time spent, and of an award under the Australian Research Grants Scheme during the remainder. Both sources of support are very gratefully acknowledged.

REFERENCES

Adamson, T. C. & Messiter, A. F. 1980 Analysis of two-dimensional interactions between shock waves and boundary layers. *Ann. Rev. Fluid Mech.* **12**, 103–138.

Dolling, D. S. & Bogdonoff, S. M. 1981 Upstream influence scaling of sharp fin-induced shock wave turbulent boundary layer interactions. *AIAA Paper* 81–0336.

Gadd, G. E. 1961 Interactions between normal shock waves and turbulent boundary layers. *ARC R & M*, 3262, 1961.

Inger, G. R. 1980 Upstream influence and skin friction in non-separating shock-turbulent boundary layer interactions. *AIAA Paper* 80–1411.

Inger, G. R. & Mason, W. H. 1976 Analytical theory of transonic normal shock-turbulent boundary-layer interaction. *AIAA J.* **14** (9) 1266–1272.

Korkegi, R. H. 1973 A simple correlation for incipient turbulent boundary-layer separation due to a skewed wave. *AIAA J.* **11** (11) 1578–1579.

KUBOTA, H. & STOLLERY, J. L. 1982 Experimental study of the interaction between a glancing shock wave and a turbulent boundary layer. *J. Fluid Mech.* **116**, 431–458.

LIGHTHILL, M. J. 1953 On boundary layers and upstream influence II. Supersonic flows without separation. *Proc. R. Soc. Lond.* A **217**, 478–507.

LIGHTHILL, M. J. 1963 Introduction to Laminar Boundary Layer Theory. In *Laminar Boundary Layers.* pp. 46–109 (ed. L. Rosenhead). Oxford University Press.

MCCABE, A. 1966 The three dimensional interaction of a shock wave with a turbulent boundary layer. *Aero. Quart.* **27**, 231–252.

MESSITER, A. F. 1980 Interaction between a normal shock wave and a turbulent boundary layer at high transonic speeds. *Z. angew. Math. Phys.* **31**, 204–226.

OSKAM, B., BOGDONOFF, S. M. & VAS, I. E. 1975 Study of the three-dimensional flow fields generated by the intersection of a skewed shock wave with a turbulent boundary layer. *AFFDL* TR–75–21.

OSKAM, B. 1976 Three-dimensional flow fields generated by the interaction of a swept shock wave with a turbulent boundary layer. *Gas Dynamics Lab. Rep.* 1313, Princeton University.

STALKER, R. J. 1958 Shock boundary layer interactions in three dimensions. PhD thesis, Dept. Aero. Eng. University of Sydney.

STALKER, R. J. 1960 Sweepback effects in a turbulent boundary-layer shock-wave interaction. *J. Aero. Sci.* **27**, 348–356.

STALKER, R. J. 1984 A characteristics approach to swept shock wave-boundary layer interactions. *AIAA J.* **22** (11), 1626–1632.

STEWARTSON, K. & WILLIAMS, P. G. 1969 Self induced separation. *Proc. R. Soc. Lond.* A **312**, 181–206.